

## Enhancement of spin accumulation in a nonmagnetic layer by reducing junction size

T. Kimura,<sup>1,2,\*</sup> Y. Otani,<sup>1,2</sup> and J. Hamrle<sup>2</sup>

<sup>1</sup>*Institute for Solid State Physics, University of Tokyo, 5-1-5 Kashiwanoha, Kashiwa, Chiba 277-8581, Japan*

<sup>2</sup>*RIKEN FRS, 2-1 Hirosawa, Wako, Saitama 351-0198, Japan*

(Received 26 January 2006; published 14 April 2006)

The junction size dependence of the spin accumulation in a nonmagnet is studied by using lateral spin valves geometry consisting of the Py/Cu ohmic junctions. We experimentally demonstrate that reducing the size of the junction drastically improves the efficiency of the spin injection into the Cu wire because of the enhancement of the spin resistance for the Py wire. The spin polarization in the Cu wire increases exponentially with reducing the junction area irrespective of the same spacing between the injector and the detector. The junction size dependence of the spin signal yields the spin diffusion lengths and the spin polarization which are reasonable values compared with previous experiments.

DOI: [10.1103/PhysRevB.73.132405](https://doi.org/10.1103/PhysRevB.73.132405)

PACS number(s): 75.75.+a, 72.25.Ba, 72.25.Mk, 75.70.Cn

Accumulation of electron spins in nonmagnets ( $Ns$ ) due to spin injection induces nontrivial properties for the new generation magnetoelectric devices.<sup>1</sup> Therefore, exploring efficient spin injection technique into  $Ns$  is a key to develop the spin information devices based on the spin-dependent transport. There are several ways to inject spins into  $Ns$  such as spin-polarized electrical current injection (electrical spin injection),<sup>2-5</sup> illumination of the circular polarized laser beam (optical spin injection),<sup>6,7</sup> magnetization precession (spin pumping),<sup>8,9</sup> etc. The electrical spin injection may be the most suitable technique for conventional electrical devices, the spin polarization in the  $N$  is detected using a ferromagnetic injector-detector geometry.<sup>10</sup> One of the most important parameters in the device is the traveling length of the electron spin, i.e., the distance between the spin injector and detector that must be shorter than the spin diffusion length of the  $N$  to induce large spin polarization. A vertical magnetic multilayered structure is thus good for inducing large spin polarization in a  $N$  because the traveling length can be tuned by setting the thickness of the  $N$  layer.<sup>11</sup> Recent nanofabrication techniques enable us to observe spin-dependent transport phenomena even in lateral  $F/N$  hybrid structures, more functional than the vertical structures.

In the lateral structures, especially in the ohmic junctions, we have to be careful about spurious magnetoresistance effects such as anisotropic magnetoresistance, the Hall effect, etc., not related to the spin accumulation in the  $Ns$ . Johnson and Silsbee first performed electrical spin injection into a  $N$  configured in a quasilateral structure and succeeded in detecting the signal due to the spin accumulation using a special potentiometric method with a nonlocal current injection.<sup>2</sup> However, the obtained signal was very small in the picovolt range because of the large sample dimensions. Jedema *et al.* have recently demonstrated a nonlocal spin valve (NLSV) measurement similar to the Johnson's potentiometric method with reducing the sample dimensions to detect the clear spin signal even at room temperature.<sup>3</sup> Thus, nonlocal current injection is an effective method for detecting the clear spin polarization induced in  $Ns$  by the electrical spin injection from  $Fs$ . In their devices, a cross-shaped Cu is often structured inbetween the ferromagnetic injector and de-

tor to obtain large spin-injection efficiency.<sup>3</sup> It is pointed out that the effective traveling length for the electron spin is given by the electrode spacing between the ferromagnetic injector and detector in the lateral spin valves (LSVs) consisting of ohmic junctions.

We have reported that the inhomogeneous current distribution in the vicinity of the ohmic junction also affects the spin signal in the lateral structures.<sup>12</sup> The spatial distribution of the spin current and accumulation can be well calculated by the spin resistance circuit model.<sup>5</sup> From the calculation, the spin accumulation and current are found to depend not only on the electrode spacing but also on the spin resistance of each consisting segment,<sup>13</sup> defined as

$$R_S = \frac{2\sigma\lambda}{(1-\alpha^2)S}. \quad (1)$$

Here,  $\lambda$ ,  $\alpha$ , and  $\sigma$  are, respectively, the spin diffusion length, the spin polarization and the conductivity.  $S$  is the cross sectional area effective for the spin current. The physical meaning of the spin resistance is a measure of the difficulty for spin mixing over the spin diffusion length. We therefore have to carefully estimate the effective cross sectional area  $S$  for the spin resistance. For the materials with long spin diffusion length more than submicrometers such as Cu, Al, and other  $Ns$ ,<sup>2,3,11</sup> The value of  $S$  should be given by the cross section of the segment which sustains the flow of the spin current. On the other hand, for the materials with short spin diffusion length of about a few nanometers such as  $Fs$ , the value of  $S$  should be given by the size of the junction in contact with other material because the spin current abruptly decays in the vicinity.<sup>5,13</sup> Therefore, the spin polarization induced in the  $Ns$  should depend on the  $F/N$  junction size. In this Brief Report, we experimentally demonstrate that the size of the ohmic  $F/N$  junction is an important geometrical factor for obtaining large spin polarization in  $Ns$  and that both the spin polarization and the spin resistance of the  $F$  are enhanced by adjusting the junction size.

The devices used for the present study is the LSVs consisting of a  $1\ \mu\text{m} \times 2\ \mu\text{m}$  Py pad 30 nm in thickness a Cu cross 80 nm in thickness, and a Py wire 100 nm in width and

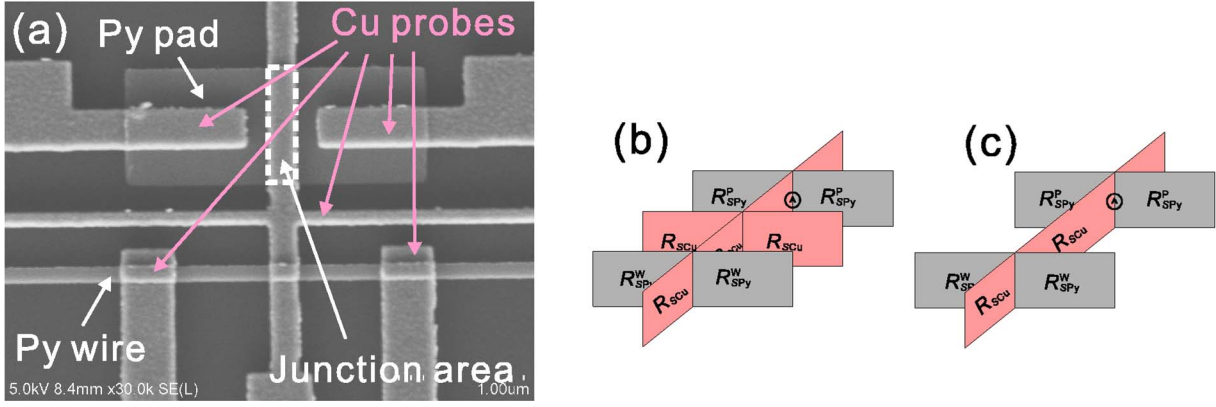


FIG. 1. (Color online) (a) The scanning electron microscope (SEM) image of the fabricated lateral spin valve with the large junction size of  $200 \text{ nm} \times 1 \text{ } \mu\text{m}$ . (b) Equivalent spin-resistance circuit and (c) a simplified one.

30 nm in thickness, [Fig. 1(a)]. The Py layer is grown using an electron-beam evaporator with a base pressure of  $2 \times 10^{-9}$  Torr. The Cu wire is evaporated by a resistance heating evaporator with a base pressure of  $3 \times 10^{-8}$  Torr. The interface between Py and Cu is well cleaned by Ar-ion milling prior to the deposition. The interface resistance is very low which assures good ohmic contact. The spacing between the Py pad and the Py wire is 600 nm. The magnetic field is applied along the easy axis of the Py wire. The resistivities of Py and Cu wires are, respectively  $10.2 \text{ } \mu\Omega \text{ cm}$  and  $1.14 \text{ } \mu\Omega \text{ cm}$  at 77 K. All the measurements are performed at 77 K by means of a conventional lock-in technique.

To begin with, we fabricated the LSV with a large junction size of  $1 \text{ } \mu\text{m} \times 200 \text{ nm}$  between the Py pads and the Cu

wire, as shown in Fig. 1(a). This device geometry is quite similar to that of the device used in Ref. 3. As mentioned above, the difference in the junction size between the injector and the detector gives rise to a significant difference in the spin resistance. We calculate the spin signal induced in the asymmetric LSV using our previous spin-resistance circuit model. In the cross-shaped Cu wire, the effective spin resistances of the vertical Cu arms are much smaller than the horizontal Cu arms because the vertical Cu arms have additional ohmic contacts with the Py pad and wire.<sup>5,14</sup> Therefore, in the calculation, we neglect the influence of the horizontal Cu arms. The spin signal of the NLSV measurement can be calculated as follows:

$$\Delta R = \frac{\alpha_{\text{Py}}^2 R_{\text{SPy}}^{\text{P}} R_{\text{SPy}}^{\text{W}} R_{\text{SCu}}}{\left\{ [R_{\text{SCu}}(R_{\text{SPy}}^{\text{P}} + R_{\text{SPy}}^{\text{W}}) + 2R_{\text{SPy}}^{\text{P}} R_{\text{SPy}}^{\text{W}}] \left[ \cosh\left(\frac{d}{\lambda_{\text{Cu}}}\right) + \sinh\left(\frac{d}{\lambda_{\text{Cu}}}\right) \right] + R_{\text{SCu}}^2 \sinh\left(\frac{d}{\lambda_{\text{Cu}}}\right) \right\}}. \quad (2)$$

Here,  $R_{\text{SPy}}^{\text{P}}$ ,  $R_{\text{SPy}}^{\text{W}}$ , and  $R_{\text{SCu}}$  are, respectively, the spin resistances of the Py pad, the Py and Cu wires.  $\alpha_{\text{Py}}$ ,  $\lambda_{\text{Cu}}$ , and  $d$  are, respectively, the spin polarization of the Py, spin diffusion length of the Cu wire and the average traveling length for the electron spin from the injector to the detector. We note that replacing  $R_{\text{SPy}}^{\text{P}}$  with  $R_{\text{SPy}}^{\text{W}}$  in Eq. (2) does not cause any change in signal.

In the NLSV measurement, there are two configurations for injecting spin current from the Py pad into the Cu wire. One is the configuration where the current is injected into the Cu cross located inbetween the Py pad and Py wire, as “injection A.” The other one is that the charge current is injected into the upper Cu wire about the Py pad, as “injection B.” The schematic illustrations corresponding to injection A and injection B are shown in the insets of Figs. 2(a) and 2(b), respectively. According to Ref. 3, injection A provides a more efficient spin injection method than injection B in the lateral ohmic junctions because the inhomogeneous current

distribution shortens the effective traveling length between the injector and the detector. The NLSV signals corresponding to injection A and injection B are shown in Figs. 2(a) and 2(b), respectively. Surprisingly, the obtained spin signals in both configurations are the same order of magnitude  $50 \text{ } \mu\Omega$ , although the background resistances originated from the charge current distribution shows the large difference. This means that both configurations exhibit the same efficiencies on the spin injection. The spin signal measured in the reverse configuration with the detector Py pad and the injector Py wire are also the same magnitude of  $50 \text{ } \mu\Omega$ . This is consistent with the reciprocity relation of Eq. (2). We note that the obtained spin signal in the present device is an order of magnitude smaller than that in the LSV consisting of two Py wires 100 nm in width with the same electrode spacing of 600 nm. Therefore, the poor spin signal in the present device is due to the small spin resistance of the Py pad. In order to

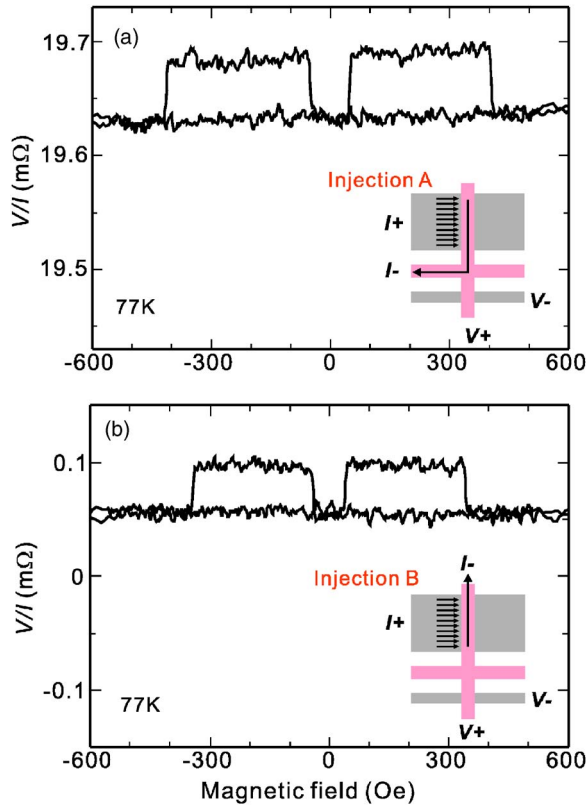


FIG. 2. (Color online) (a) Nonlocal spin valve signal of the large-junction device with the injection A configuration. (b) Nonlocal spin valve signal with the injection B configuration. The insets in each figure show the corresponding probe configurations.

perform the efficient spin injection, the spin resistance of the Py pad has to be large.

As mentioned above, reducing the size of the ohmic junction between the Py pad and the Cu wire increases the spin resistance of the Py pad. The size of the junction area can be reduced by cutting the Cu wire on the Py pad, as seen in the inset of Fig. 3(a). Here, the junction size is  $200 \text{ nm} \times 200 \text{ nm}$ . The electrode spacing between the injector and the detector is 600 nm, the same as that in the previous device mentioned above. In this device, only the probe configuration of injection A is effective in detecting the spin signal. Injection B is ineffective because the upper Cu wire about the Py pad is not directly connected with the Cu wire on the Py wire. The spin signal of  $0.12 \text{ m}\Omega$  in Fig. 3(a) is twice as large as that of the previous device with the same electrode spacing. This supports that the reduction of the junction size raises the spin resistance of the Py wire. We further reduce the junction size between the Py pad and the Cu wire. Figures 3(b) and 3(c) show the observed NLSV signals with the junction sizes of  $60 \text{ nm} \times 200 \text{ nm}$  and  $30 \text{ nm} \times 200 \text{ nm}$ , respectively. We can clearly confirm that the spin signal is increased by reducing the junction size. For example, the spin signal in Fig. 3(c) is enhanced ten times more than that in Fig. 2 with keeping the electrode spacing 600 nm.

The spin signal is plotted as a function of the junction size in Fig. 4. The signal exponentially increases with reducing the junction size. The measured spin signals are fitted to Eq. (2). Since the difference between the spin resistances  $R_{SPy}^P$  for

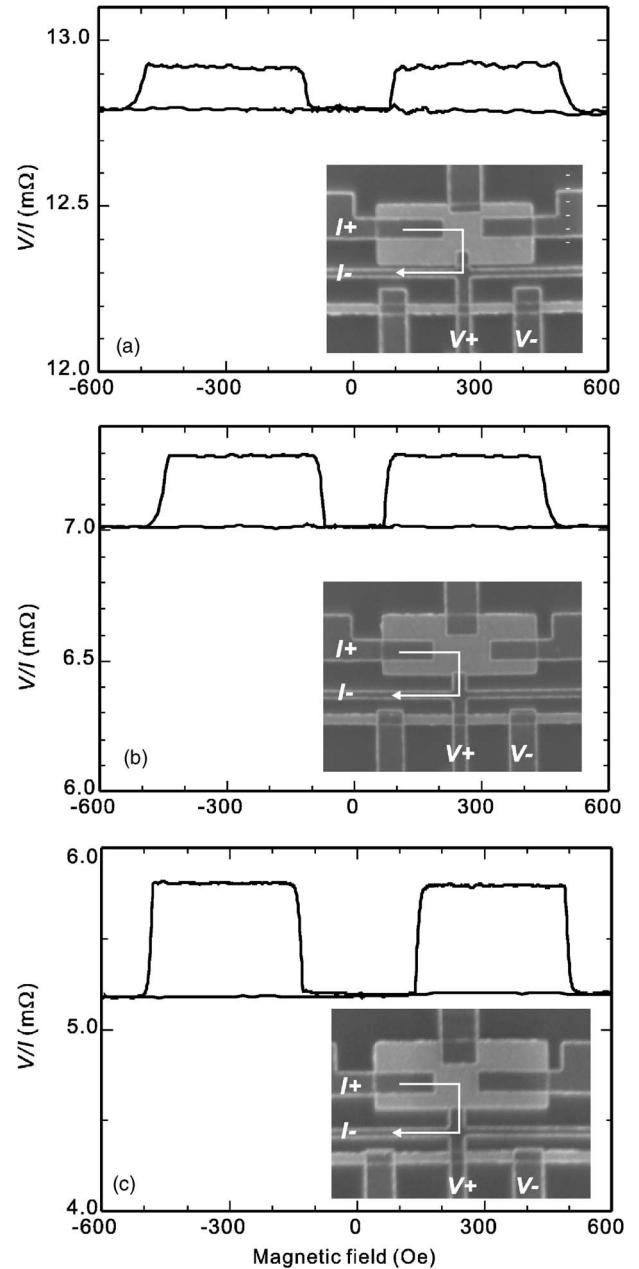


FIG. 3. Nonlocal spin valve signals measured for devices with different junction sizes of (a)  $200 \text{ nm} \times 200 \text{ nm}$ , (b)  $60 \text{ nm} \times 200 \text{ nm}$ , and (c)  $30 \text{ nm} \times 200 \text{ nm}$ . The insets of each figure show the SEM images with the probe configurations.

the Py pad and that  $R_{SPy}^W$  for the Py wire is only in the effective cross section  $S$ , we assume the relation  $R_{SPy}^P = [(l_w w)/(l_p w)] R_{SPy}^W$ . Here,  $w$  is the width of the Cu probe, 200 nm in the present case,  $l_w$  is the width of the Py wire, 100 nm in the present case, and  $l_p$  is the contact length of the Cu wire on the Py pad. The effective traveling length  $d$  for the electron spin is assumed to be given by  $l_p/2 + l_w/2 + d_{sp}$ , which is the center-center distance between the injector and the detector. Here,  $d_{sp}$  is the electrode spacing between the Py pad and the Py wire, 600 nm in the present case. The fitted curve well reproduces the experimental results. From the fitting parameters, we obtain the spin resistances of the Cu wire and the Py wire as  $2.14 \Omega$  and  $0.08 \Omega$ , respectively.

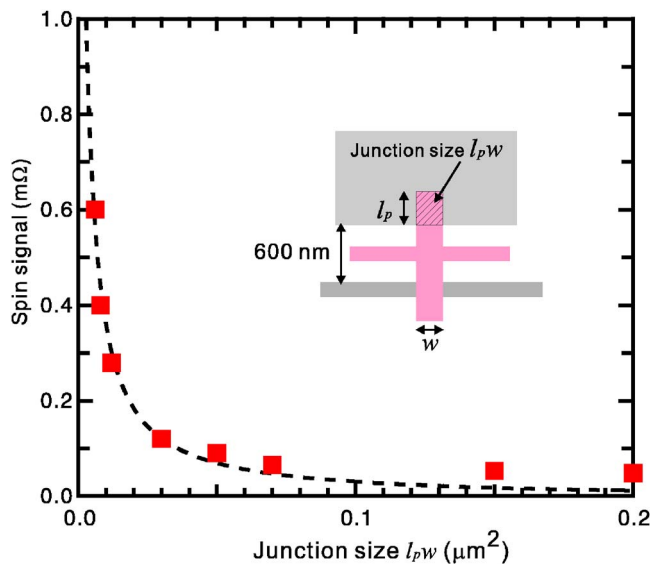


FIG. 4. (Color online) Spin signal in the NLSV measurement as a function of the junction size  $l_p w$ . The dotted curve is the best fitting to the data points using Eq. (2).

The spin diffusion length of the Cu wire is found to be  $1.5 \mu\text{m}$  at 77 K, longer than the values in Refs. 3 and 15. This indicates that our Cu wire has better quality than others. The spin polarization and the spin diffusion length of the Py

wire are respectively 0.25 and 3.5 nm, reasonable values compared with previous experiments.<sup>3,5,16</sup>

In the former study,<sup>3</sup> the magnitude of the spin signal is independent of the size of the  $F/N$  junction and depends only on the electrode spacing between the detector and the injector in the similar LSVs consisting of Py/Cu ohmic junctions. At present, we do not understand this discrepancy which may be caused by the difference of the thicknesses of Py and Cu wires. In their devices, the thickness of the Cu is 50 nm, and is slightly thicker than the 40 nm of the Py pad. This may connect the Cu wire to the Py pad only at the edge. In that case, the effective traveling length of the electron spin should be given by the electrode spacing. The difference in the quality of the interface between the present and former devices may be related to this discrepancy. We should note that our results are well described by considering the diffusive transport with ideal transparent interfaces.<sup>13</sup>

In conclusion, we have experimentally demonstrated that the size of the  $F/N$  junction is an important geometrical factor to obtain large spin-injection efficiency in the LSVs. The spin polarizations in the Cu wires are enhanced drastically by reducing the size of the junction between Py and Cu with keeping the electrode spacing between the injector and detector. The junction size dependence of the spin signal yields the spin diffusion lengths and the spin polarization which are reasonable values compared with previous experiments. This result provides a method for the efficient spin injection to develop future spintronic devices.

\*Electronic address: kimura@issp.u-tokyo.ac.jp

- <sup>1</sup>I. Žutić, J. Fabian and S. Das Sarma, Rev. Mod. Phys. **76**, 323 (2004).
- <sup>2</sup>M. Johnson and R. H. Silsbee, Phys. Rev. Lett. **55**, 1790 (1985).
- <sup>3</sup>F. J. Jedema, A. T. Filip, and B. J. van Wees, Nature (London) **410**, 345 (2001).
- <sup>4</sup>G. Schmidt, D. Ferrand, L. W. Molenkamp, A. T. Filip, and B. J. van Wees, Phys. Rev. B **62**, R4790 (2000).
- <sup>5</sup>T. Kimura, J. Hamrle, and Y. Otani, Phys. Rev. B **72**, 014461 (2005).
- <sup>6</sup>J. M. Kikkawa, I. P. Smorchkova, N. Samarth, and D. D. Awschalom, Science **277**, 1284 (1997).
- <sup>7</sup>A. Oiwa, Y. Mitsumori, R. Moriya, T. Slupinski, and H. Munekata, Phys. Rev. Lett. **88**, 137202 (2002).
- <sup>8</sup>S. Mizukami, Y. Ando, and T. Miyazaki, Phys. Rev. B **66**, 104413 (2002).

- <sup>9</sup>Y. Tserkovnyak, A. Brataas, and G. E. W. Bauer, Phys. Rev. B **66**, 224403 (2002).
- <sup>10</sup>G. E. W. Bauer, A. Brataas, Y. Tserkovnyak, and B. J. van Wees, Appl. Phys. Lett. **82**, 3928 (2003).
- <sup>11</sup>W. P. Pratt, Jr., S.-F. Lee, J. M. Slaughter, R. Loloee, P. A. Schroeder, and J. Bass, Phys. Rev. Lett. **66**, 3060 (1991).
- <sup>12</sup>T. Kimura, J. Hamrle, and Y. Otani, J. Appl. Phys. **97**, 076102 (2005).
- <sup>13</sup>S. Takahashi and S. Maekawa, Phys. Rev. B **67**, 052409 (2003).
- <sup>14</sup>T. Kimura, J. Hamrle, Y. Otani, K. Tsukagoshi, and Y. Aoyagi, Appl. Phys. Lett. **85**, 3795 (2004).
- <sup>15</sup>F. J. Albert, N. C. Emley, E. B. Myers, D. C. Ralph, and R. A. Buhrman, Phys. Rev. Lett. **89**, 226802 (2002).
- <sup>16</sup>S. Dubois, L. Piraux, J. M. George, K. Ounadjela, J. L. Duvail, and A. Fert, Phys. Rev. B **60**, 477 (1999).